

Magnetic field distribution in ferromagnetic metal/normal metal multilayers using NMRJ. Lu, P. L. Kuhns, M. J. R. Hoch, W. G. Moulton, and A. P. Reyes
National High Magnetic Field Laboratory, Tallahassee, Florida 32310, USA

(Received 7 March 2005; revised manuscript received 26 May 2005; published 2 August 2005)

The origin of the interlayer exchange coupling in ferromagnetic-normal metal (FM-NM) multilayer structures has been the focus of intensive research efforts for more than a decade. NMR is an important method for investigating these systems. We have studied room temperature molecular-beam-epitaxy grown Co/Al and Fe/Cu multilayer structures using ^{59}Co , ^{27}Al , and ^{63}Cu nuclei as probes. The ^{59}Co FM-NMR results for Co/Al films indicate about 3 ML of Co is intermixed with Al at the interface. For both Co/Al and Fe/Cu samples substantial NM line broadening is observed with no indication of line structure or splitting. The line broadening increases with decrease of the NM layer thickness. The Ruderman-Kittel-Kasuya-Yosida (RKKY)-like interaction across the interface was investigated using a Fe/Cu sample with an insulating AlO_x layer separating each Fe layer from adjacent Cu layers. Our ^{63}Cu results for this sample are very similar to results obtained without the insulating oxide barrier. This shows that the line broadening is not due to the RKKY-like interaction but interfacial roughness. Simulation of the local internal magnetic field using a simple rough interface model provides support for this suggestion.

DOI: [10.1103/PhysRevB.72.054401](https://doi.org/10.1103/PhysRevB.72.054401)

PACS number(s): 75.70.Cn, 75.30.Et, 76.60.Jx

I. INTRODUCTION

Since the discovery of interlayer exchange coupling (IEC),¹ a large number of experimental and theoretical investigations of the nature and properties of this coupling have been carried out.²⁻⁵ The magnetic coupling between two ferromagnetic (FM) layers separated by a normal metal (NM) layers oscillates between parallel and antiparallel with increase in thickness of the NM layer, characterized by a typical period of 10 \AA .^{1,2} This oscillation in the coupling persists for up to 5 periods (50 \AA). The origin of this oscillation has been considered to be a Ruderman-Kittel-Kasuya-Yosida (RKKY)-like interaction via conduction electrons of the NM layer.^{3,4} Another theoretical model involves confinement effects in spin dependent quantum wells formed in the NM layers.⁵ These models both suggest that in the NM layer, the electron spins are spatially polarized in an oscillatory pattern.

Hyperfine couplings allow the spatial electron spin polarization in a NM layer, adjacent to a FM layer, to be probed via Knight shifts. In principle, the spatial oscillation of the electron spin polarization in the NM layer will result in either NMR line broadening or discrete secondary spectral components in addition to the main NMR line. For example, additional Cu NMR peaks have been reported in diluted Fe-Cu and Co-Cu systems.⁶ The additional lines were assigned to RKKY interactions with up to 4th nearest neighbor of the transition-metal ion.

Few NMR results for NM layers in FM/NM multilayer systems have been published.^{7,8} Jin *et al.*⁷ have reported up to 12 additional ^{63}Cu NMR lines in Fe/Cu multilayers at room temperature. They attribute these lines to a RKKY-like interaction with an estimated oscillation period of 4 \AA . However, no explanation is given for the intensity of the additional lines and no attempt made to fit the line separations with RKKY-like oscillations. Furthermore, no dependence of the spectra on Cu layer thickness is shown. Yasuoka and Goto,⁸ in a ^{63}Cu NMR study of Ni/Cu multilayers, found

significant line broadening without additional spectral components. They attribute the observed line broadening and the line shape changes with magnetic field orientation to a RKKY-like interaction. The absence of discrete spectral features is explained by assuming that the RKKY oscillations in different regions have different phases due to interface roughness. The choice of the Ni/Cu system in their work can cause complications, because Ni and Cu are miscible even at room temperature according to the Ni-Cu binary phase diagram.⁹ The possibility that the NMR line broadening is due to Ni-Cu intermixing at the interfaces needs to be considered. Recent work on Al thin films sputtered on Co films suggests that the ^{27}Al NMR line broadens due to the stray magnetic field produced by interfacial roughness.¹⁰

While the primary objective of this work is to investigate the RKKY interaction in the NM layers, Co FM-NMR is used to characterize the multilayer structure especially in the interface region. There are a number of publications on similar systems in the literature.¹⁰⁻¹⁵

The work presented here is a systematic NMR investigation of interlayer magnetic couplings in MBE grown Co/Al and Fe/Cu multilayers, as a function of NM thickness. A specific goal is to determine the role and importance, if any, of RKKY interactions in systems of this kind.

II. EXPERIMENT

The samples were grown in an EPI MBE system equipped with Fe, Co electron beam sources, and Al, Cu effusion cells. The purity of source materials are Fe 99.98%, Co 99.999%, Al 99.999%, and Cu 99.95%. The MBE chamber base pressure was 5×10^{-9} Torr. The layer thickness was monitored *in situ* by a quartz crystal thickness monitor (QCM) placed near the sample. The QCM was calibrated by *ex situ* film thickness measurement using atomic force microscopy (AFM). The typical growth rates were $\sim 1.0 \text{ \AA/s}$ for Fe, Co, Al and $\sim 0.3 \text{ \AA/s}$ for Cu. The substrates were semi-insulating

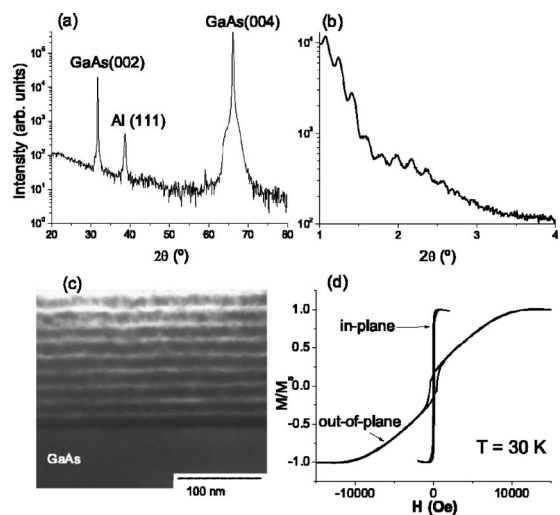


FIG. 1. Representative characterizations of the multilayer samples. (a) Low angle XRD and (b) XRD θ - 2θ scan of Co/Al = [60 Å/500 Å] × 3. (c) XTEM bright field images of Co/Al = [60 Å/150 Å] × 9, the bright bands are Al layers. (d) The magnetic hysteresis loops of Co/Al = [20 Å/40 Å] × 25 measured at 30 K.

GaAs(001) for Co/Al and *n* type Si(001) for Fe/Cu. The substrates were solvent cleaned before loading into the MBE system. All samples were grown at room temperature (with no temperature regulation). The substrate temperature increased by $\sim 20^\circ\text{C}$ during growth due to the radiation from the sources. For the ^{59}Co experiment, a sample of Co/Al = [20 Å/40 Å] × 50 was grown. For both the Co/Al and Fe/Cu multilayers, the Co and Fe layer thickness was fixed at 60 Å. The Al thickness values were 25 Å, 50 Å, 75 Å, 150 Å, 250 Å, and 500 Å, while the Cu thickness values were 25 Å, 100 Å, 200 Å, 300 Å, and 600 Å. The total Al or Cu thickness in each multilayer sample was made roughly the same for NMR sensitivity reasons. After growth, sample surfaces were painted with photoresist to prevent film oxidation before the measurements were made.

X-ray diffraction (XRD) θ - 2θ scan, low angle x-ray scattering, transmission electron microscopy (TEM), atomic force microscopy (AFM), and superconducting quantum interference device magnetometry (SQUID) were used to characterize the films. XRD θ - 2θ patterns of our samples show that the Al in Co/Al and Cu in Fe/Cu are both (111) textured polycrystalline [Fig. 1(a)]. Low angle XRD for both Co/Al and Fe/Cu multilayer systems gives clear oscillations indicating reasonably flat interfaces [Fig. 1(b)]. The typical surface average roughness for films of total thickness of ~ 1500 Å was about 9 Å as measured by AFM. Cross-sectional TEM revealed the evolution of the interface roughness with thickness [Fig. 1(c)]. As expected, the substrate interface is very flat, but the film surface roughness increases with increasing film thickness. Representative magnetic hysteresis loops are shown in Fig. 1(d) for the applied field both parallel and perpendicular to the film. The marked difference between the two loops is due to the magnetic shape anisotropy as expected for magnetic thin films.

NMR experiments were performed with a pulsed NMR spectrometer. For ^{59}Co zero external field FM-NMR, the

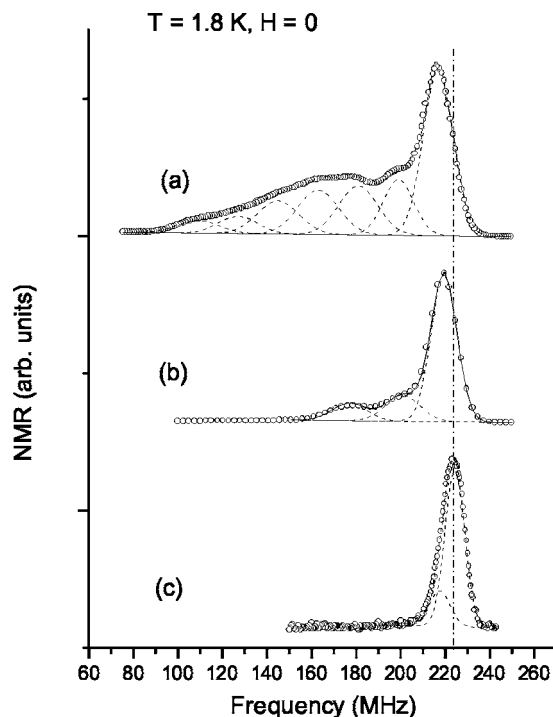


FIG. 2. FM-NMR ^{59}Co spectra of (a) MBE grown Co/Al = [20 Å/40 Å] × 25, (b) MBE grown Co/Ag = [20 Å/20 Å] × 20, and (c) sputtered 400 Å Co film.

large FM enhancement factor allowed use of an untuned probe, configured to have $Q \approx 1$ using a 50 Ohm load, providing a flat frequency response across the frequency sweep range. For Co FM-NMR of a multilayer structure, the enhancement factor may vary across the spectrum necessitating a correction for this effect.¹⁰⁻¹⁵ For our Co/Al and Co/Ag samples, we have measured the enhancement at several frequencies [140 (Co/Al only), 180, and 217 MHz] to be the same within 20%. For the semiquantitative ^{59}Co FM-NMR work presented here, the spectrum is not corrected for this small enhancement frequency dependence. For ^{63}Cu NMR using a tuned probe, care was taken to minimize background Cu signals from the probe. An empty probe field-sweep experiment showed the background ^{63}Cu signal to be at least one order of magnitude lower than the signal from the samples. The NMR sample size was $\sim 5 \times 5$ mm². To increase the signal-to-noise ratio in some cases, substrates were mechanically thinned to < 100 μm after the films were grown and a few pieces cut from the same large sample were stacked. For all the NMR experiment, spin echo methods were used. NMR spectra were analyzed by summing individual Fourier transforms at different frequencies or fields.

III. RESULTS AND DISCUSSION

A. ^{59}Co FM-NMR

Figure 2(a) shows the ^{59}Co FM-NMR spectrum of a Co/Al = [20 Å/40 Å] × 50 sample at 1.8 K. For comparison, Fig. 2(b) shows the spectrum of Co/Ag = [20 Å/20 Å] × 20 film, and Fig. 2(c) that of a single layer 400 Å dc-sputtered

Co film. The ^{59}Co line for the single 400 Å Co film can be fit with two peaks centered at 224 MHz and 217.4 MHz consistent with hcp Co and fcc Co respectively¹² indicating mixed hcp and fcc phases with hcp being the majority phase. The main ^{59}Co lines of Co/Al and Co/Ag are found at frequencies close to the ^{59}Co resonance frequency of fcc Co indicating that most of the Co in both films is the fcc phase. For Co/Al and Co/Ag samples, we attribute the shoulders at lower frequency to the resonance from the ^{59}Co near the interface. It is well established that at interfaces replacing each Co atom with a nonmagnetic atom reduces the hyperfine field for the neighboring Co atoms. This effect shifts the ^{59}Co resonance frequency for such regions down by about 16–19 MHz.^{11,12} Co/Al and Co/Ag zero-field NMR spectra were fit with multiple Gaussian functions separated by ~ 18 MHz as plotted in dash lines in Fig. 2. The fitting result indicates that Co/Ag has relatively small interfacial mixing, and Co atoms at Co/Ag interfaces predominantly have only 1 or 2 missing nearest neighbors. For Co/Al, however, there are significant contributions to the spectrum from Co atoms with 3, 4, 5, and 6 substituted nearest neighbors, revealing considerably more intermixing at the Co/Al interfaces than at the Co/Ag interfaces. From the ratio of areas between the fitted main peak and all the shoulder peaks combined, it is estimated that the interface region of Co/Al involves a mixture of Co and Al with thickness ~ 6 Å (~ 3 ML of Co). In contrast, the Co/Ag interface region only has a thickness ~ 2 Å (~ 1 ML of Co) indicating a sharp interface. Small errors in this semiquantitative estimate may come from the signal enhancement frequency dependence as explained above. In addition it is possible that a small number of Co atoms in the interface region become paramagnetic and therefore do not contribute to the spectrum. The 3 ML of intermixing at the Co/Al interface is in good agreement with Rutherford backscattering spectrometry and x-ray photoemission spectroscopy results obtained in a previous study of a Co film grown on Al at room temperature.¹⁶ The difference in the interface quality between Co/Al and Co/Ag multilayers can be understood from the Al-Co and Ag-Co binary phase diagrams. The Al-Co system has a few equilibrium intermetallic phases at 200 °C, while Ag and Co are almost immiscible even at much higher temperatures.⁹

B. ^{27}Al and ^{63}Cu NMR

The ^{27}Al spectra of Co/Al samples with Co thickness of 60 Å, and various Al thickness values, are shown in Fig. 3. In this experiment, the magnetic field was swept, stepwise, through the resonance keeping the RF frequency fixed at 127 MHz. The magnetic field was directed perpendicular to the film plane. The strong narrow line at the center of each spectrum is a marker from bulk Al metal. For samples with Al thickness 25 Å, 50 Å, and 75 Å, the resonance peak (not shown) is so broad that the signal is hardly discernable from the background noise even following considerable data averaging. As the Al layer thickness is increased, the linewidth decreases. However, even for 500 Å Al, the maximum thickness used, the linewidth is a factor of 10 greater than that of pure Al films. This considerable line broadening cannot be

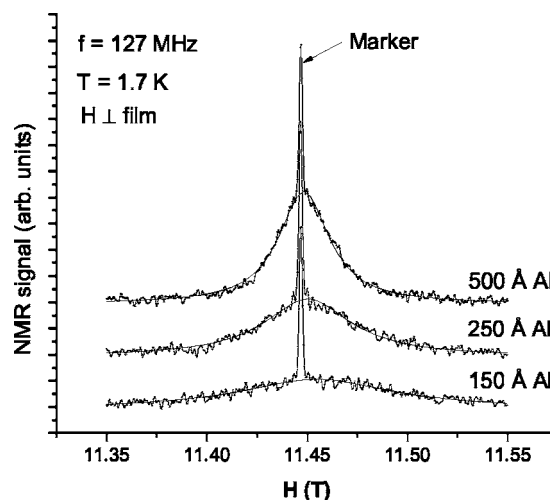


FIG. 3. ^{27}Al NMR spectra of Co/Al multilayer samples with the same Co thickness but different Al thickness: Co/Al = [60 Å/150 Å] \times 9, Co/Al = [60 Å/250 Å] \times 6, and Co/Al = [60 Å/500 Å] \times 3. The lines are guides to the eye.

accounted for by interfacial mixing of Al and Co, since the ^{59}Co FM-NMR indicates the intermixing region in Co/Al is only ~ 3 ML, so for a 500 Å Al layer the intermixing effect is negligible.

In order to further explore interfacial mixing and other NMR line-broadening effects, the Fe/Cu system has been investigated. According to the Cu-Fe phase diagram⁹ Cu and Fe are immiscible even in the liquid phase. Interfacial intermixing can be therefore ruled out as the predominant broadening mechanism. A ^{63}Cu spectrum of an Fe/Cu = [60 Å/25 Å] \times 50 sample was obtained in an effort to reproduce the results of Ref. 7. This experiment was performed with the magnetic field in the plane of the film. The line was extremely broad and no splitting or structure was observed in the spectrum. Figures 4(a) and 4(b) show NMR spectra of Fe-Cu multilayers with different Cu thickness. The linewidth decreases with increasing Cu thickness, but appreciable line broadening compared to the Cu/Ag multilayers is evident even at Cu thickness of 600 Å (not shown here). While this is similar to our Co/Al NMR data, it is quite different from the result of Ref. 7 where multiple ^{63}Cu lines are shown. It is also noted that the center of the spectrum for Fe/Cu = [60 Å/100 Å] \times 9 [Fig. 4(c)] is shifted to a lower field compared to the other two spectra.

Some contribution to ^{63}Cu ($I=3/2$) and ^{27}Al ($I=5/2$) line broadening might arise from quadrupolar splitting due to Cu and Al layer structural imperfections such as strain, grain boundaries and dislocations. It is also possible that size effects may play a role. There has been a report of considerable Cu NMR line broadening for nanometer size Cu particle samples.¹⁷ To check on these possibilities, we have grown Ag/Cu = [60 Å/300 Å] \times 6, i.e., replaced Fe with Ag while keeping all other growth parameters unchanged. The ^{63}Cu NMR linewidth of Ag/Cu is much narrower than that of the corresponding Fe/Cu spectrum [Fig. 4(b)] as shown in Fig. 4(c). Assuming the Cu layer crystalline quality is similar in both Ag/Cu and Fe/Cu films, this indicates that the major

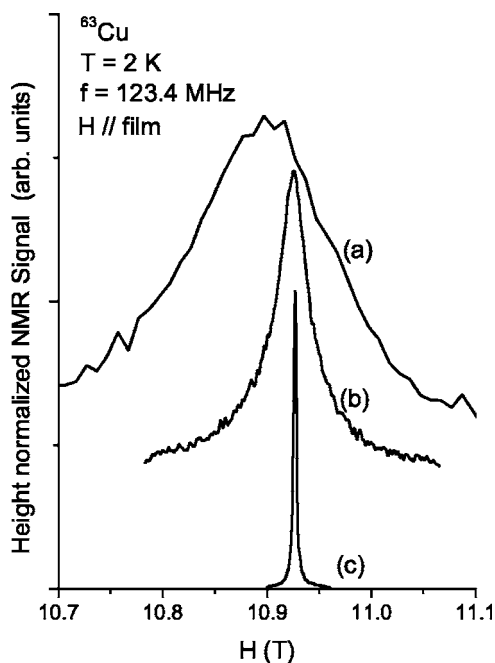


FIG. 4. ^{63}Cu NMR spectra of Fe/Cu multilayer samples with the same Fe thickness but different Cu thickness. (a) Fe/Cu = [60 Å/100 Å] × 9, (b) Fe/Cu = [60 Å/300 Å] × 5, and (c) a control sample Ag/Cu = [60 Å/300 Å] × 5.

contribution to the line broadening is not related to crystal-line quality or size effects in the Al or Cu layers.

To test the hypothesis that the major contributor to the broadening might be due to a RKKY-like interaction, a [60 Å Fe/15 Å AlO_x /200 Å Cu/15 Å AlO_x] × 6 multilayer sample was grown. The RKKY-like interaction should be substantially suppressed by an insulating AlO_x layer between each Fe and Cu layer. The ^{63}Cu spectral width should therefore be reduced if any significant part of the line broadening is caused by a RKKY-like interaction. Each AlO_x layer was grown by depositing 15 Å Al, then naturally oxidizing the metal at room temperature in 5 psi of pure oxygen for 30 minutes. The inset of Fig. 5 is a TEM image of the cross section of this sample. High resolution TEM (not shown) reveals amorphous structure of the AlO_x layers. As may be seen in Fig. 5, the ^{63}Cu spectra show a very small difference in linewidth between the samples with and without AlO_x (Fig. 5) showing that the major line broadening effect is not of RKKY origin. The small difference in linewidths can be explained by the difference in sample roughness as will be discussed below.

The central peak positions of both Al and Cu lines shift towards higher magnetic field when H_0 is perpendicular to the films, compared to the parallel field configuration. The shift increases as the Al or Cu thickness is reduced. This shift cannot be accounted for in any straightforward way by either roughness or a RKKY-like interaction. Because of the differences in FM material used and the sample preparation details, a direct quantitative comparison of our results to the results obtained for Ni/Cu system in Ref. 8 is not considered here.

Interface roughness is an important issue in understanding magnetic properties of magnetic thin films. For most of the

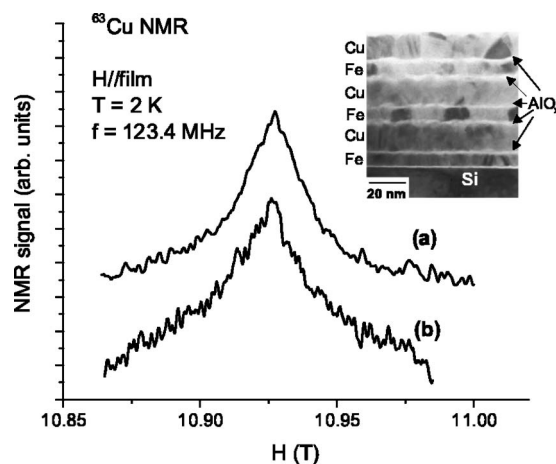


FIG. 5. ^{63}Cu NMR spectra of Fe/Cu multilayers with (a) and without (b) AlO_x insulating layer. The layer structure of Fe/Cu with insulating AlO_x is depicted in the inset.

metal multilayer films, it is very difficult to obtain an atomically flat interface and it is difficult to control the film roughness. The “stray field” from rough FM layers can cause a nonuniform magnetic field distribution in the NM layers. To roughly estimate the “stray field” in the NM layers, we have used a simple model as depicted in Fig. 6(a). For convenience the interfacial roughness is chosen to have square wave form with height h , wavelength λ , and infinite extent in the y direction perpendicular to the paper. The NM layer has thickness t . When the magnetization of the FM layer is saturated, the surface density of induced magnetic charge on the side walls of the square wave is the saturation magnetization M_s . The “stray field” H_s at a given point $P(x_0, y_0, z_0)$ within the shaded area is the sum of the contribution from all the magnetic charge,

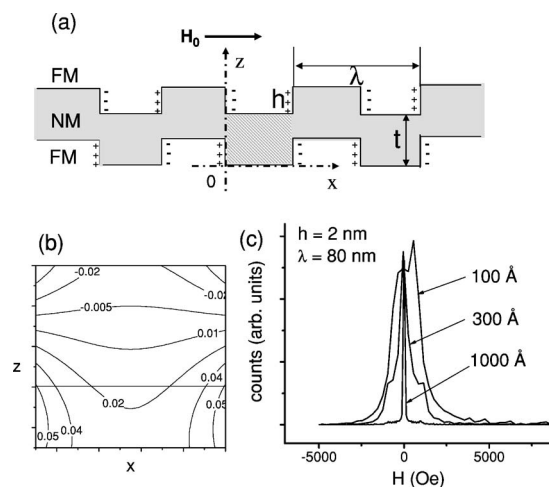


FIG. 6. (a) Schematic of the roughness model. (b) The calculated stray field distribution in the shaded area of (a) in tesla. (c) Histograms obtained from the calculated stray field distribution based on the model in (a). The histograms shown are height normalized for the same roughness parameters with different normal metal layer thickness of 100, 300, and 1000 Å, respectively. The roughness parameter h and λ are chosen to be typical values for our samples as measured by AFM.

$$H_s = \sum_w \frac{\mu_0}{4\pi} \iint \frac{x_0 - x_w}{r^3} M_s dydz, \quad (1)$$

where $r = \sqrt{(x-x_0)^2 + (y-y_0)^2 + (z-z_0)^2}$, and x_w is the x position of a “side wall.” Integrating y from $-\infty$ to $+\infty$ and z from 0 to h , gives

$$H_s = \sum_w \frac{\mu_0}{4\pi} \left[\tan^{-1} \frac{h - z_0}{x_0 - x_w} - \tan^{-1} \frac{-z_0}{x_0 - x_w} \right]. \quad (2)$$

To a good approximation, we can take the sum over the “side walls” within 2λ of the area of interest [shaded area in Fig. 6(a)]. The distribution of “stray field” in the shaded area of Fig. 6(a) was calculated and is shown in a contour map for realistic roughness parameters: $t=10$ nm, $\lambda=40$ nm, and $h=2$ nm in Fig. 6(b). Because of the geometrical symmetry of the model, the field distribution of the entire NM layer is the repetition of that in the shaded area. The histogram of the “stray field” distribution in the shaded area corresponds to the NMR line shape. Figure 6(c) shows three calculated histograms corresponding to three different NM layer thickness values with the same roughness parameters. The decreased line broadening, due to the surface roughness, with increasing NM layer thickness is evident. This admittedly oversimplified model is qualitatively consistent with our experimental observations. The asymmetry of the simulated line for 100 Å film is in agreement with the line shift observed in Fe/Cu films [Fig. 4(b)].

IV. CONCLUSIONS

Co/Al and Fe/Cu multilayer thin films were grown using MBE and characterized using XRD, TEM, SQUID, and AFM. ^{59}Co , ^{27}Al , and ^{63}Cu NMR was used to study the Co/Al and Fe/Cu multilayer structures. For the Co/Al system interfacial intermixing extending over ~ 3 ML is found from the ^{59}Co FM-NMR measurements. In the NM layers, considerable ^{27}Al and ^{63}Cu NMR line broadening is observed with decrease of the Al (in Co/Al) and Cu (in Fe/Cu) layer thickness. In contrast to previous ^{63}Cu NMR of Fe/Cu multilayers, no additional ^{63}Cu peaks or features are found in our Fe/Cu samples. Using a sample with a 15 Å insulating AlO_x layer between each Cu and Fe layer it has been shown that a RKKY-like interaction is not responsible for this broadening. This finding contrasts with previous work on similar systems. It is suggested that the line broadening is due to the “stray-field” distribution from the rough FM/NM interface. This conclusion is supported by simulations using a simple surface roughness model.

ACKNOWLEDGMENTS

The authors would like to thank Dr. Y. Xin for TEM measurements. This work is financially supported by The Defense Advanced Research Projects Agency (DARPA) grant MDA972-03-01-0010. Partial support by the National Science Foundation under cooperative agreement No. DMR-0084173 and the State of Florida is gratefully acknowledged.

- ¹S. S. P. Parkin, N. More, and K. P. Roche, *Phys. Rev. Lett.* **64**, 2304 (1990).
- ²S. S. P. Parkin, R. Bhadra, and K. P. Roche, *Phys. Rev. Lett.* **66**, 2152 (1991).
- ³P. Bruno and C. Chappert, *Phys. Rev. Lett.* **67**, 1602 (1991).
- ⁴M. D. Stiles, *Phys. Rev. B* **48**, 7238 (1993).
- ⁵J. Mathon, Murielle Villeret, R. B. Muniz, J. d’Albuquerque e Castro, and D. M. Edwards, *Phys. Rev. Lett.* **74**, 3696 (1995).
- ⁶D. V. Lang, J. B. Boyce, D. C. Lo, and C. P. Slichter, *Phys. Rev. Lett.* **29**, 776 (1972); D. C. Lo, D. V. Lang, J. B. Boyce, and C. P. Slichter, *Phys. Rev. B* **8**, 973 (1973); J. B. Boyce and C. P. Slichter, *Phys. Rev. Lett.* **32**, 61 (1974).
- ⁷Q. Y. Jin, Y. B. Xu, H. R. Zhai, C. Hu, M. Lu, Q. S. Bie, Y. Zhai, G. L. Dunifer, R. Naik, and M. Ahmad, *Phys. Rev. Lett.* **72**, 768 (1994).
- ⁸H. Yasuoka and A. Goto, *Mater. Sci. Eng., B* **31**, 177 (1995).
- ⁹*Binary Alloy Phase Diagrams*, 2nd ed., edited by T. B. Massalski (ASM International, Materials Park, OH, 1990).
- ¹⁰H. A. M. de Gronckel, H. Kohlstedt, and C. Daniels, *Appl. Phys. A: Mater. Sci. Process.* **70**, 435 (2000).

- ¹¹H. A. M. de Gronckel, K. Kopinga, W. J. M. de Jonge, P. Panissod, J. P. Schille, and F. J. A. den Broeder, *Phys. Rev. B* **44**, 9100 (1991).
- ¹²C. Meny, P. Panissod, and R. Loloee, *Phys. Rev. B* **45**, 12269 (1992); C. Meny, E. Jedryka, and P. Panissod, *J. Phys.: Condens. Matter* **5**, 1547 (1993).
- ¹³E. A. M. van Alphen and W. J. M. de Jonge, *Phys. Rev. B* **51**, 8182 (1995); E. A. M. van Alphen, S. G. E. te Velthuis, H. A. M. de Gronckel, K. Kopinga, and W. J. M. de Jonge, *Phys. Rev. B* **49**, 17336 (1994).
- ¹⁴T. Thomson, P. C. Riedi, Q. Wang, and H. Zabe, *J. Appl. Phys.* **79**, 6300 (1996); T. Thomson, P. C. Riedi, and D. Greig, *Phys. Rev. B* **50**, 10319 (1994).
- ¹⁵C. Christides, S. Stavroyiannis, D. Niarchos, M. Wojcik, S. Nadolski, and E. Jedryka, *Phys. Rev. B* **59**, 8812 (1999).
- ¹⁶N. R. Shivaparan, M. A. Teter, and R. J. Smith, *Surf. Sci.* **476**, 152 (2001).
- ¹⁷D. P. Tunstall, P. P. Edwards, J. Todd, and M. J. Williams, *J. Phys.: Condens. Matter* **6**, 1791 (1994).